Journal of Alloys and Compounds 542 (2012) 293–297

Contents lists available at SciVerse ScienceDirect

Journal of Alloys and Compounds

journal homepage: www.elsevier.com/locate/jalcom

Influence of La^{3+} and Fe^{3+} co-doping to nano-TiO_2 prepared by graded calcination

Zhe Yang, Jing-tang Zheng *, Ming-bo Wu

The State Key Laboratory of Heavy Oil, China University of Petroleum, Dongying, Shandong 257061, China

ARTICLE INFO

Article history:
Received 14 February 2012
Received in revised form 6 April 2012
Accepted 4 May 2012
Available online 12 May 2012

Keywords:
TiO_2
Graded calcinations
Photocatalytic activity
Co-doping
La^{3+}
Fe^{3+}

ABSTRACT

The un-doping, single-doping and co-doping TiO_2 nanoparticles have been prepared through the graded calcination method with $Ti(OC_4H_9)_4$ as raw material and characterized by X-ray diffraction (XRD) and UV–vis reflection spectra. Their photocatalytic activities have been investigated by the photocatalytic oxidation of methyl orange. It is indicated that Fe^{3+}-doping makes the reflection profile narrow, improves photoutilization of TiO_2, and then generates more electron–hole pairs. La^{3+}-doping restrains the increase of grain size, leads to crystal expansion plus matrix distortion and retards the recombination of the photoexcited charge carriers. The photocatalytic activity of TiO_2 co-doped with La^{3+} and Fe^{3+} is notably improved due to the cooperative actions of the two dopants.

© 2012 Published by Elsevier B.V.

1. Introduction

The photocatalytic oxidation of organic compounds using semiconductor catalysts (i.e. TiO_2), has been extensively studied in recent years [1,2]. Nano-TiO_2 is opening a new way for the treatment of environment pollution because of its relatively low cost, non-toxicity, chemical stability and recyclability. Furthermore, it could degrade refractory organics into non-toxic CO_2, H_2O or some other simple inorganic compounds [3–7]. However, TiO_2 utilizes only a very small fraction of the solar spectrum due to its band-gap energy. Meanwhile, the photocatalytic activity of TiO_2 is limited by fast charge-carrier recombination and low interfacial charge-transfer rates of photogenerated carriers [8]. Many researches have been carried out in order to improve the photocatalytic activity of TiO_2 through expanding absorption band edge of titania (shown as blue shift [9] or red shift). Previous researches [10–20] indicated that one of effective ways is introducing two or more proper elements into nanocrystalline TiO_2 particles. Some indicate that co-doping transition metal ions and rare earth metal into the nanocrystalline TiO_2 may have a synergistic effect, which could increase the activity of TiO_2.

In this work, co-doping TiO_2 using Fe^{3+} and La^{3+} was prepared by the graded calcination method. The photocatalytic activity was then evaluated by photodegradation of methyl orange in solution. It is shown that the co-doping of Fe^{3+} and La^{3+}, compared with un-doping TiO_2 and single-doping, can obviously enhance the photocatalytic activity in the methyl orange degradation test under visible light irradiation. The synergistic effect of two dopants resulting in the enhancement of photodegradation has also been discussed.

2. Experimental

2.1. Graded calcination synthesis of doping TiO_2

At present, many researchers have used sol–gel method for the preparation of TiO_2. However, in order to improve the photocatalytic activity of TiO_2 prepared by sol–gel method [21,22], several days even several weeks had to be spent in gelling (Fig. 1). A new method called graded calcination, which shortened the time for sol translating into dry gel to 6 h with acceptable photocatalytic activity of TiO_2, was developed to resolve the problem in this research.

All reagents used in the experiment are analytically pure. A solution of $Ti(OC_4H_9)_4$, in two-thirds anhydrous ethanol, was used as molecular precursor of TiO_2. Acetic acid was used as a chemical additive to moderate the reaction rate. The distilled water was used for hydrolysis in solution with $Ti(OC_4H_9)_4$ and one-thirds anhydrous ethanol was added gradually under magnetic stirring at room temperature. After the ultrasonic oscillation (Frequency: 25 kHz) of sols, the temperature of water-bath was raised to 80 °C and kept 6 h for obtaining dry gels. The resulting dry gels were triturated in a mortar, and then calcined in a tube furnace with N_2 at 400 °C for 2 h to give intermediate powder, the powder form was showed in Fig. 2(a). Finally, the resulting powder was calcined in a box resistance furnace with O_2 at 500 °C for 2 h to gain TiO_2 sample which was showed in Fig. 2(b). Doping TiO_2 nanoparticles were synthesized by using almost the same method. The appropriate amount of $Fe(NO_3)_3{\cdot}9H_2O$ or $La(NO_3)_3{\cdot}6H_2O$ was dissolved in anhydrous ethanol, which was added to the distilled water prior to the hydrolysis of $Ti(OC_4H_9)_4$. For convenience, the samples were labeled as TF(X), TL(Y) for Fe^{3+} and La^{3+} doping TiO_2, and TF(X)L(Y) for Fe^{3+} and La^{3+} co-doping TiO_2, where X and Y referred to the nominal atomic concentration of Fe^{3+} and La^{3+}, respectively.

2.2. Characterization

The concentration of methyl orange in solution was measured with a spectrophotometer (DR/2500). X-ray diffraction (XRD) patterns of all samples were obtained with a X'pert PROMPD diffractometer (Cu Kα radiation, $\lambda = 1.5406$ Å)

* Corresponding author. Tel.: +86 546 8395024; fax: +86 546 8395190.
E-mail address: jtzheng03@163.com (J.-t. Zheng).

0925-8388/$ - see front matter © 2012 Published by Elsevier B.V.
http://dx.doi.org/10.1016/j.jallcom.2012.05.028

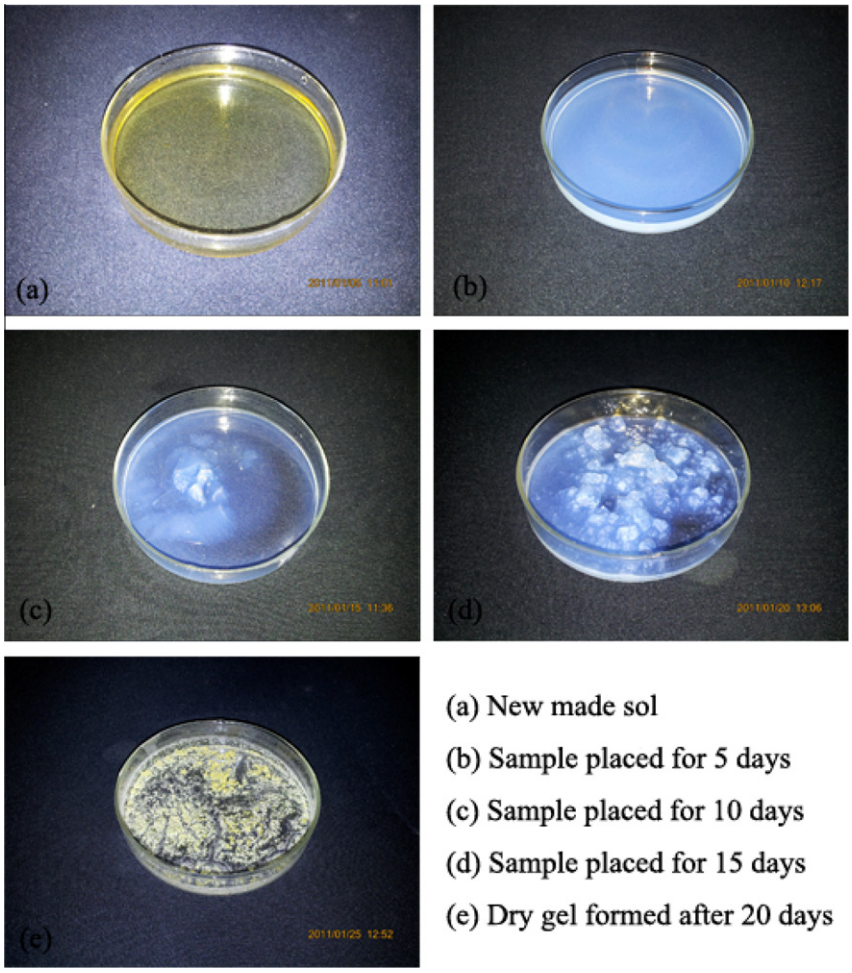

Fig. 1. Gel process of the sample by sol–gel method.

which was produced by Holand PANalytical Company. UV–Vis reflection spectra (DRS) of samples were recorded on UV-3000 spectrophotometer. High pure $BaSO_4$ was used as a standard reagent.

2.3. Measurement of photocatalytic efficiency

The photoreaction was carried out in a 500 mL cylindrical vessel with a water-cooled quartz jacket. Irradiation was provided by a 1000 W high pressure xenon lamp as visible light. A magnetic stirrer was equipped at the bottom of the reactor to achieve effective dispersion. Air was bubbled through the reaction solution from the bottom to ensure a constant dissolved O_2 concentration. Pure TiO_2 powder was also tested to assess the photocatalytic activity of doping TiO_2. The concentration of sample chosen was 2 g/L. The initial methyl orange concentration was 20 mg/L and 500 mL methyl orange solution was used for the photocatalytic degradation each time. The temperature of the reaction solution was maintained at 30 ± 0.5 °C. Some reactive solutions were withdrawn at different intervals. The residual concentration of methyl orange was measured at 465 nm with a DR/2500 spectrophotometer.

3. Experimental results and discussion

3.1. Photocatalytic activity

The photocatalytic activity of the samples was measured by using the degradation of aqueous solution of methyl orange as reference (without concerning the degradation intermediates). Before irradiated under visible light, the samples were stirred in darkness for 0.5 h. Detection results showed that the methyl orange concentration negligibly decreased, which was caused by the slight absorption on photo-catalysts surface. It indicated that there was no degradation in the absence of irradiation.

In order to find the doped TiO_2 with optimizing photocatalytic activity, the photocatalytic oxidation of methyl orange under visible light was implemented to test the photocatalytic performance of pure TiO_2, single doped TiO_2 with La^{3+} or Fe^{3+}, and the co-doped TiO_2 with La^{3+} and Fe^{3+}, respectively. The selected doping ratio of Fe^{3+} was 0, 0.05%, 0.1% and 0.5%, respectively, while La^{3+} was 0, 0.05%, 0.1% and 0.5%, respectively. The evolutions of methyl orange photodegradation as a function of irradiation time are presented in Fig. 3. As can be seen in Fig. 3, the photocatalytic activity of TF(0.05)L(0.1) was stronger than that of other samples under visible light. In comparison with pure TiO_2, doping TiO_2 has higher photo-catalytic activity. Compared with un-doping and single-doping, the co-doping of Fe^{3+} and La^{3+} can notably enhance the photocatalytic activity of TiO_2. The improvement suggests that there exists a synergistic effect on the catalytic activity when both Fe^{3+} and La^{3+} are co-doped into the nanocrystalline TiO_2 particles.

3.2. X-ray diffraction

X-ray diffraction measurements (as shown in Fig. 4) indicate that all samples prepared have the anatase structure. The more broadening of X-ray diffraction peaks is observed obviously in TL(0.1) samples than that observed in un-doping sample. (103), (004) and (112) peaks of anatase are conjoint, which results in a

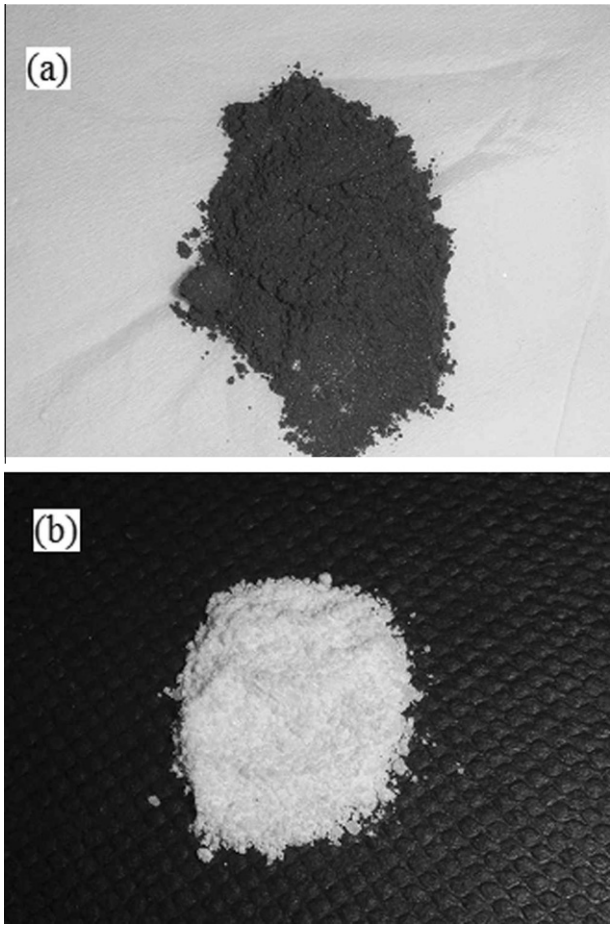

Fig. 2. The appearance of the TiO_2 sample. (a) Sample form of intermediate product; (b) end product of TiO_2 sample.

broad diffraction peak. (105) and (211) XRD peaks also trend to conjoin together. The X-ray diffraction peaks of TF(0.05) samples are similar to that of un-doping sample. The broad degree of peaks in TF(0.05)L(0.1) is between them. No characteristic peak of iron oxide or lanthanum oxide is found in the XRD patterns, which either means that Fe^{3+} and La^{3+} ions are incorporated in the crystallinity of TiO_2 or implies that iron oxide and lanthanum oxide are very small and highly dispersed [23].

The average grain size is calculated on the basis of the broadening of the (101) XRD peak of anatase by using Scherrer equation: $D = K\lambda/(\beta\cos\theta)$. The distortion of the TiO_2 matrices was also estimated from the XRD spectra by using the equation: $\varepsilon = \beta/4tg\theta$. The particle characteristics of the samples used in this study are summarized in Table 1. The crystallite size decreases for the doping. It indicates that Fe^{3+} or La^{3+} doping restrains the increase of grain size and refines crystallite size. The change of crystal parameters of the doping samples becomes great, compared with that of un-doping samples. It is suggested that crystal matrix could be expanded. The matrix distortion increases in the order of TiO_2, TF(0.05), TF(0.05)L(0.1) and TL(0.1). According to Pauling's principle, it is easy for Fe^{3+} ion to cooperate with the matrix of the TiO_2 nano particles without causing much crystalline distortion. However, the substitution of La^{3+} into the matrix of TiO_2 would affect the coordination number and distort the matrix. So the distortion of TL(0.1) is maximum, while that of TF(0.05) is minimum. The distortion of TF(0.05)L(0.1) lies between them.

Both Fig. 4 and Table 1 show that the lattice distortion of La^{3+} and Fe^{3+} co-doping TiO_2 has been enhanced. The expansion of the crystal matrix creates oxygen vacancies, which generates shallow energy states at the bottom of the conduction band and are served as electron trap site in the nanocrystalline TiO_2. Meanwhile, shallow energy states introduced by rare earth ion at the top valence band are served as hole trap sites. The separation of the charge carriers is attributed to such trapping. Subsequently, the charge carriers transfer to the surface of photocatalyst and initiate redox reactions. The photocatalytic activity of doping TiO_2 is thus promoted.

When both Fe^{3+} and La^{3+} are co-doped into the nanocrystalline TiO_2 particles, a cooperative operation would be produced. Fe^{3+}-doping broadens the absorption profile, improves photo utilization of TiO_2, and then generates more electron–hole pairs. La^{3+}-doping restrains the increase of grain size, leads to crystal expansion and matrix distortion and retards the recombination of the photoexcited charge carriers. The photocatalytic activity of TiO_2 co-doped with Fe^{3+} and La^{3+} is thus notably improved.

3.3. UV–vis reflection spectra

Fig. 5 shows the UV–vis reflection spectra of Fe^{3+} and La^{3+} co-doping and un-doping TiO_2, respectively. Compared with the spectrum of pure titania, a tiny blue-shift of the absorption profile and a obvious red-shift are clearly observed in the spectrum of co-doping TiO_2. The reflection of visible light region of the co-doping TiO_2 of Fe^{3+} and La^{3+} is weakened (as can be seen in Fig. 4). It shows that co-doping of Fe^{3+} and La^{3+} improves photo-utilization of TiO_2 and generates more electron–hole pairs under photo irradiation in visible light region, which helps to improve the photocatalytic activity of TiO_2.

4. Conclusions

The graded calcination method offer successful routes to synthesize doping TiO_2 catalysts. Fe^{3+}-doping broadens the absorption profile, improves photo utilization of TiO_2, and then generates more electron–hole pairs. La^{3+}-doping restrains the increase of grain size, leads to crystal expansion and matrix distortion and retards the recombination of the photoexcited charge carriers. The photocatalytic activity of TiO_2 co-doped with both Fe^{3+} and La^{3+}

Table 1
XRD analysis results of samples.

Sample	Percent content (%)		Crystal size (nm)	Matrix distortion ε (%)
	Anatase	Rutile		
TiO_2	100	–	17.8	0.5216
TF(0.05)	100	–	13.0	1.2040
TL(0.1)	100	–	12.2	1.2809
TF(0.05)L(0.1)	100	–	16.0	1.2278

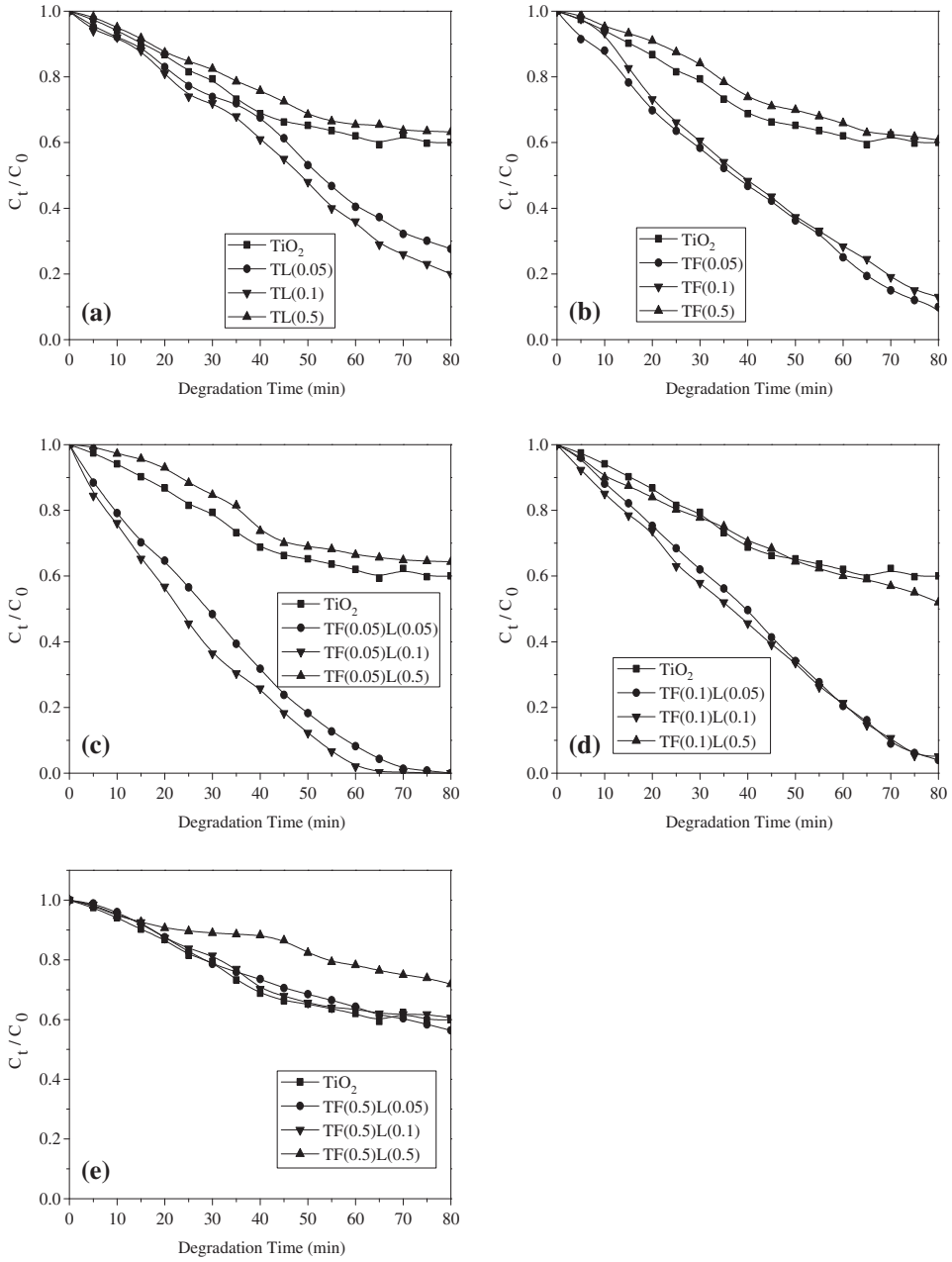

Fig. 3. Degradation curves of methyl orange as a function of irradiation time.

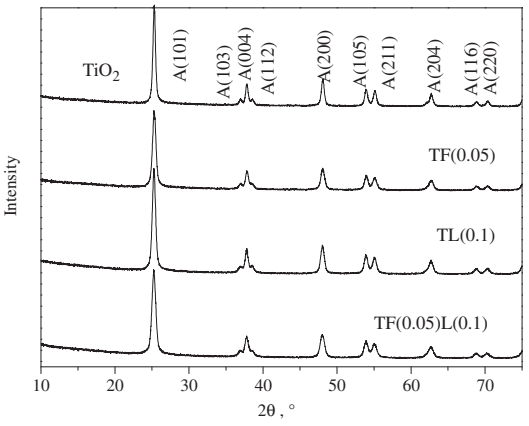

Fig. 4. XRD patterns of samples (A – anatase).

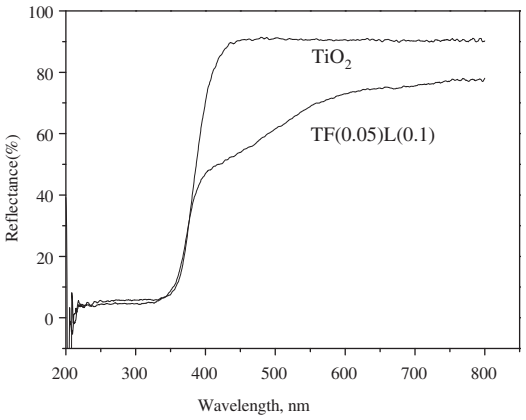

Fig. 5. UV–vis reflection spectra of samples.

ions is markedly improved due to the cooperative actions of the two dopants. It may be expected that photocatalytic activity can be further improved by choosing proper dopants.

Acknowledgements

This work has been supported by the National Basic Research Program of China (2011CB605703), the National Natural Science Foundation of China (Nos. 20976196 and 21176260), the Natural Science Foundation of Shandong (ZR2009FL028) and the Fundamental Research Funds for the Central Universities (09CX05009A).

References

[1] M. Grätzel, Nature 414 (2001) 338–344.
[2] A. Mills, S.L. Hunte, J. Photochem. Photobiol. A 108 (1997) 1–35.
[3] Y.H. Tseng, C.S. Kuo, C.H. Huang, T. Hirakawa, N. Negishi, H.L. Bai, Micro Nano Lett. 5 (2010) 81–84.
[4] R.J. Tan, Y.H. Tseng, C.H. Kuo, Micro Nano Lett. 5 (2010) 361–364.
[5] Y.H. Tseng, C.Y. Yen, M.Y. Yen, C.C.M. Ma, Micro Nano Lett. 5 (2010) 1–6.
[6] Y. Djaoued, K. Ozga, A. Wojciechowski, A.H. Reshak, J. Robichaud, I.V. Kityk, J. Alloys Comp. 508 (2010) 599–605.
[7] H.A. Monreal, J.G. Chacon-Nava, U. Arce-Colunga, C.A. Martinez, P.G. Casillas, A. Martinez-Villafane, Micro Nano Lett. 4 (2009) 187–191.
[8] A.C. Zaman, C.B. Üstündağ, F. Kaya, C. Kaya, Mater. Lett. 66 (2012) 179–181.
[9] P. Karasinski, E. Gondek, S. Drewniak, et al., J. Sol–Gel Sci. Technol. 61 (2012) 355–361.
[10] S. Sakthivel, B. Neppolian, M.V. Shankar, B. Arabindoo, M. Palanichamy, V. Murugesan, Sol. Energy Mater. Sol. Cells 77 (2003) 65.
[11] C. Wang, H. Shang, Y. Tao, T. Yuan, G. Zhang, Sep. Purif. Technol. 32 (2003) 357.
[12] H.J. Tang, M. Zhang, Z.J. Cao, L.Y. Ye, Glass Enamel 31 (2003) 20–25.
[13] X.Q. Chen, J.Y. Yang, X.Y. Jiang, J.F. Song, Chin. J. Appl. Chem. 1 (2003) 73–76.
[14] S.H. Xu, F.L. Shen, Chinese Rare Earths 31 (2010) 89–92.
[15] X.Y. Yang, J. Luo, D.L. Li, Adv. Mater. Res. 113-116 (2010) 1945–1950.
[16] Z.L. Shi, X.X. Zhang, S.H. Yao, Particuology 9 (2011) 260–264.
[17] T. Wang, Y.Y. Wang, Z.J. Han, Appl. Chem. Ind. 37 (2008) 1786–1793.
[18] X.Q. Chen, J.Y. Yang, J.S. Zhang, J. Central South Univ. Technol. 11 (2004) 161–165.
[19] Q.Q. Wang, S.H. Xu, F.L. Shen, Appl. Surf. Sci. 257 (2011) 7671–7677.
[20] L.S. Yin, J. Zhu, L.S. Wen, S. Yang, Q.X. Xie, World Sci. Tech. R. D. 30 (2008) 122–125.
[21] Kanakkanmavudi B. Jaimy, Swapankumar Ghosh, Sasidharan Sankar, K.G.K. Warrier, Mater Res. Bull. 46 (2011) 921–924.
[22] H. Krüger, A. Hertwig, U. Beck, E. Kemnitz, Thin Solid Films 518 (2010) 6080–6086.
[23] J.C.S. Wu, C.H. Chen, J. Photochem. Photobiol. A. Chem. 163 (2004) 509.